# Electroexcitation of giant electric-dipole and electric-quadrupole resonances in $^{42}$Ca and $^{44}$Ca

K. Itoh and Y. M. Shin

*Saskatchewan Accelerator Laboratory, University of Saskatchewan, Saskatoon*
*S7N 0W0, Canada*

T. Saito and Y. Torizuka

*Laboratory of Nuclear Science, Tohoku University, Mikamine, Sendai 982, Japan*

(Received 18 February 1981)

We present the giant electric-dipole and electric-quadrupole cross sections of $^{42}$Ca and $^{44}$Ca measured by inelastic electron scattering with incident energies between 124 and 250 MeV. Spectra were decomposed into dipole, quadrupole, and other higher multipole components. The giant dipole resonances in both nuclei have a large width of approximately 12 MeV, with at least two gross resonance structures. The quadrupole resonances are distributed in several clusters between 10 and 22 MeV, depleting $(61\pm9)\%$ in $^{42}$Ca and $(46\pm7)\%$ in $^{44}$Ca of the isoscalar energy-weighted sum rule, respectively. Higher multipole resonances were also found in the same excitation energy region. The observed structure in the dipole and quadrupole resonances are examined in terms of the collective model, and it is suggested that the splitting of the dipole resonance revealed in $^{44}$Ca may reflect the effect of nuclear deformation.

> NUCLEAR REACTIONS $^{42}$Ca $(e,e')$ and $^{44}$Ca $(e,e')$, $E=124\sim250$ MeV, $q=0.4\sim1.2$ fm$^{-1}$, enriched target, measured $\sigma(E',\theta)$ up to 35 MeV in excitation energy; deduced electric-dipole, electric-quadrupole, and higher multipole strength in the giant resonance region.

## I. INTRODUCTION

The giant electric-dipole and electric-quadrupole resonances (GDR and GQR) in the doubly magic $^{40}$Ca nucleus have been studied quite extensively through photonuclear reactions,[1,2] inelastic electron scattering,[3] and inelastic hadron scattering[4] such as $(\alpha,\alpha')$, $(p,p')$, etc. However, little is known about the giant multipole resonances in other calcium isotopes.

Recently, measurements of the $^{42}$Ca $(\gamma,p)$,[5,6] $^{42}$Ca$(\gamma,n)$,[7] and $^{44}$Ca$(\gamma,p)$ (Ref. 8) cross sections have been performed by the Tohoku and Melbourne groups. One of the interesting features of these cross sections is that the photoneutron cross sections increase rapidly with increasing neutron number, contrary to the photoproton cross sections. Also, the peak positions of $(\gamma,n)$ cross sections were observed generally several MeV lower than those of $(\gamma,p)$ cross sections. Furthermore,

the two gross peaks of the GDR have been observed in $^{42}$Ca and $^{44}$Ca by the $^{41}$K$(p,\gamma_0)^{42}$Ca (Ref. 9) and $^{44}$Ca$(\gamma,p_0)$ (Ref. 8) reactions. Their results indicate that the peak positions are roughly in accord with the isospin splitting theory[10] but the strengths of the peaks assigned as $T_>$ ($T$-upper) states at 20.4 MeV in $^{42}$Ca and at 21.3 MeV in $^{44}$Ca were too strong to be explained by the theory.

According to the inelastic scattering of hadron experiments,[4,11] the GQR in $^{40}$Ca is centered at 18 MeV, depleting about a half of the isoscalar energy-weighted sum rule (EWSR). The result of the electron scattering experiment,[3] however, showed a much broader GQR in $^{40}$Ca. The isoscalar GQR's in $^{42}$Ca and $^{44}$Ca were measured very recently by the inelastic scattering of $^6$Li particles,[12] and $K$ splitting due to the nuclear deformation was suggested.

In the present work the inelastic electron scattering from $^{42}$Ca and $^{44}$Ca in the region of giant reso-

nance was studied over a wide momentum transfer range in order to identify and measure the GDR and GQR strengths in the calcium isotopes. The experimental results have been analyzed by the method of multipole expansion,[13,14] and various multipole cross sections have been obtained. A very preliminary result for $^{44}$Ca has been given in Ref. 15.

## II. EXPERIMENT AND ANALYSIS

The present experiment is an extension of the study of the giant multipole resonances in $^{40}$Ca (Ref. 3) and was performed using electron beams from the 300 MeV electron linear accelerator of Tohoku University. Self-supporting metallic targets of $^{42}$Ca and $^{44}$Ca were used. The target thicknesses of isotopically enriched $^{42}$Ca (94.4%) and $^{44}$Ca (98.6%) were 48.9 and 44.3 mg/cm$^2$, respectively. Inelastically scattered electrons were detected at forward angles by a 100 cm radius double focusing magnetic spectrometer equipped with 33 channel solid state detectors.[16] The incident beam energies and scattering angles used in this experiment were 150 MeV (35°), 183 MeV (35°), and 250 MeV (35°, 45°, 55° ) for $^{42}$Ca; 124 MeV (35°), 150 MeV (35°), 183 MeV (35°), and 250 MeV (35°, 42°, 50° ) for $^{44}$Ca. These energies and angles provided momentum transfers ranging from 0.4 to 1.2 fm$^{-1}$. Scattered electron spectra were measured up to 35 MeV in excitation energy, with an overall experimental energy resolution of 0.12%.

The measured spectra were unfolded for radiative corrections using the same iterative method used for $^{40}$Ca.[3] The radiation tail was calculated using the peaking approximation, including a radiation process proportional to the square of the target thickness.[17] The elastic cross sections of $^{42}$Ca and $^{44}$Ca at various incident electron energies were included in the tail function and the elastic form factors were obtained by the phase shift calculation,[18] adopting a three-parameter charge distribution for the ground state.[19] The cross section was obtained by comparison with the elastic scattering cross section[20] of $^{12}$C.

In the first order Born approximation it is well known that the form factor of a state is given by

$$|F(q)|^2 = \frac{d\sigma}{d\Omega}/\sigma_M$$

$$= \frac{q_\mu^4}{q^4}|F_L(q)|^2 + \left[\frac{q_\mu^2}{2q^2} + \tan^2\frac{\theta}{2}\right]|F_T(q)|^2,$$

(1)

where $\sigma_M$ is the Mott cross section for a point charge $Ze$ including the recoil factor, $F_L(q)$ and $F_T(q)$ are the longitudinal and transverse form factors, respectively, $q_\mu$ is the four momentum transfer while $q$ denotes the three momentum transfer, and $\theta$ is the scattering angle of the outgoing electrons. If the measurements were made at forward angles as in the present experiment, the transverse form factor contributes little to the measured cross section and analysis of the experimental data becomes easier since only the longitudinal form factor $F_L(q)$ is dealt with.

For continuum states it is convenient to introduce a longitudinal differential form factor in excitation energy $\omega$ defined by

$$|W_L(q,\omega)|^2 = \frac{d^2\sigma}{d\Omega d\omega}/\sigma_M$$

(2)

and

$$|F_L(q)|^2 = \int |W_L(q,\omega)|^2 d\omega.$$

(3)

If the observed resonance consists of unresolved states of different multipole excitations, then the observed form factor is an algebraic sum of the form factors belonging to the multipole excitations involved in the reaction, i.e.,

$$|F_L(q)|^2 = \sum_l |F_L^l(q)|^2$$

$$= \sum_l \int |W_L^l(q,\omega)|^2 d\omega,$$

(4)

where $l$ denotes the multipole order.

In general, the differential form factor for an $l$-pole excitation may be written as a product of two functions,[21,22] one which depends on the momentum transfer $q$, the other on the excitation energy $\omega$:

$$|W_L(q,\omega)|^2 = \sum_l |W_L^l(q,\omega)|^2$$

$$= \sum_l f_l(q)g_l(\omega),$$

(5)

where $g_l(\omega)$ could be represented by a Lorentzian or a Breit-Wigner shape for a well defined resonance. Thus, if the $q$ dependence of the $l$-pole excitation $f_l(q)$ is known for each $l$ then the energy dependence $g_l(\omega)$ can be obtained from the observed inelastic electron spectra. Conversely, if $g_l(\omega)$ is known, then $f_l(q)$ can be determined. In practice, however, neither $g_l(\omega)$ nor $f_l(q)$ for $^{42}$Ca and $^{44}$Ca is known, and one must assume the functional form of either one of these two functions for each $l$.

In the present analysis, the $q$ dependence of the electric-dipole resonance $f_1(q)$ was taken from the Goldhaber-Teller model as in the analysis of $^{40}$Ca.[3] This choice was based on the fact that not only does it explain the giant dipole resonance reasonably well,[23] but also its predictions are supported by a microscopic model calculation.[24] For higher multipole excitations the Tassie model was used. In these models the transition charge density is given by

$$\rho_{tr}(r) = r^{l-1}\frac{d}{dr}\rho_{gr}(r), \qquad (6)$$

where

$$\rho_{gr}(r) = \rho_0\{1 + \exp[(r - c_{tr})/(t_{tr}/4.40)]\}^{-1}.$$

The ground state parameters $c_0 = 3.60$ fm and $t_0 = 2.50$ fm (Ref. 25) were used as $c_{tr}$ and $t_{tr}$ for the dipole (C1) and for the quadrupole (C2) excitations. These parameters also describe very well the first diffraction pattern of the first $2^+$ state in $^{42}$Ca.[26] The parameters used for the $C3$ excitation were $c_{tr} = 0.89c_0$ and $t_{tr} = 0.91t_0$, while those for $C5$ were $c_{tr} = 0.82c_0$ and $t_{tr} = 0.75t_0$. These values are the same as those for the first $3^-$ and $5^-$ state in the $^{40}$Ca and $^{42}$Ca.[24,26] For the $C4$ and $C6$ excitation $c_{tr} = 0.95c_0$ and $t_{tr} = 0.95t_0$ were used so that the calculated form factor reproduces the experimental point[27] at $q = 1.9$ fm$^{-1}$ when all multipole excitations up to $l = 6$ are included in the analysis.

Since the number of data sets is limited, the decomposition of the differential form factor $|W_L(q,\omega)|^2$ into all the multipole components $g_l(\omega)$ loses its physical significance. Therefore each spectrum was decomposed into three contributions—the dipole, the quadrupole, and the sum of all multipole transitions higher than the octupole excitations up to and including $l = 6$. For the $q$ dependence of the composite form factor $f_l(q)$ for $l \geq 3$, the relative contribution of each multipole ($3 \leq l \leq 6$) was obtained by assuming that each multipole transition exhausts both the isoscalar and isovector energy-weighted sum rule given by[28]

$$S_l = \int \omega_l B(Cl,\omega_l)d\omega$$

$$= \frac{l(2l+1)^2}{4\pi}\frac{\hbar^2}{2M}Ze^2\langle r^{2l-2}\rangle, \qquad (7)$$

where

$$\langle r^{2l-2}\rangle = \int_0^\infty r^{2l-2}\rho_{gr}(r)d\vec{r},$$

and $\int$ denotes the sum for all discrete states and integrals for continuum states. If the eigenfrequencies $\omega_l$ of the higher multipole resonances are known, then $B(Cl)$ can be obtained. In the present analysis the resonance energies of the higher multipole excitation ($l \geq 3$) were taken from the prediction of the hydrodynamic model[29] that the resonance energy increases with increasing multipolarity.

Finally, a small correction due to transverse excitation contributions in the observed spectra was made before applying the method described above. Since in the present experiment the transverse excitation contribution was not measured, it was assumed that the transverse spectra and the form factor are the same as those measured for $^{40}$Ca.[30] The effect due to the difference of the transverse excitation between the isotopes on the extracted multipole strength is estimated to be less than 1%, because most of the transverse strength comes from the continuum spectra, and the cross section of the quasielastic scattering is proportional to $Z\mu_p^2 + N\mu_N^2$.[31] The measured transverse spectra of $^{40}$Ca in the giant resonance region are well approximated within a statistical error by

$$|W_T(q,\omega)|^2 = (a\omega + b)f_T(q). \qquad (8)$$

The values of $a$ and $b$ obtained by fitting the data for $^{40}$Ca and used in the present analysis are given in Table I. The measured $|F_T(q)|^2$ which is shown in Fig. 1 seems to peak at $q \approx 0.7$ fm$^{-1}$. After subtracting the contribution of the transverse part, the inelastic electron spectrum was divided into small energy intervals $\Delta\omega = 350$ keV and the measured differential form factor between $\omega$ and $\omega + \Delta\omega$ at a momentum transfer $q$ was expanded according to Eq. (5). The data at different $q$'s thus provided a set of parametric equations for $g_l(\omega)$'s and a $\chi^2$ fit yielded $g_l(\omega)$ for each $l[ = 1,2,\Sigma(l \geq 3)]$.

### III. RESULTS

The total form factors for $^{42}$Ca and $^{44}$Ca which are obtained by integrating from $\omega = 10$ to 25 MeV are shown in Fig. 1 together with the previous results of $^{40}$Ca (Ref. 3) and $^{48}$Ca.[27] The transverse form factor of $^{40}$Ca as well as the calculated electric-dipole transverse form factor using the wave function of the particle-hole model[32] is also shown in the same figure for comparison.

The effects of the higher multipole excitations on the extraction of dipole and quadrupole transition strengths have been investigated by varying the
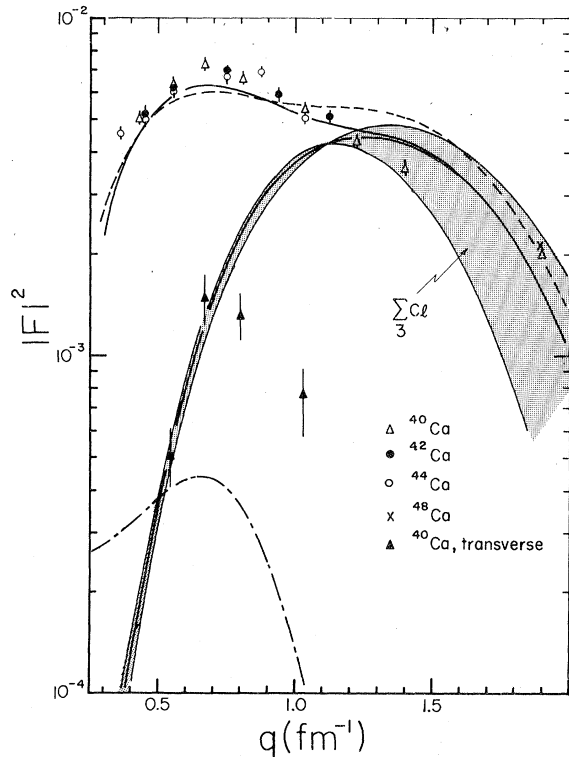
FIG. 1. The total form factor integrated from 10 to 25 MeV for $^{42}$Ca and $^{44}$Ca, together with the experimental results of $^{40}$Ca (Ref. 3). The measured form factors at $q = 1.9$ fm$^{-1}$ are taken from Ref. 27. The shaded area labeled $\Sigma Cl$ $(l \geq 3)$ is the investigated range of the contributions of the higher multipole excitation for $^{42}$Ca. The solid and dashed curves are the sum of the all multipole excitations in $^{42}$Ca and $^{44}$Ca, respectively. Also the measured transverse form factor of $^{40}$Ca integrated in the same energy range is shown. The electric-dipole transverse form factor calculated using the particle-hole wave functions (Ref. 32) is shown by the dot-dashed curve.

parameters $c_{tr}$ and $t_{tr}$ in Eq. (6) from $0.90c_0$ and $0.90t_0$ to the full values of $c_0$ to $t_0$, the range of which should be sufficient for the inelastic electron scattering process for the calcium isotopes for the $q$ range currently investigated.[24] At the same time the position of the $l$-pole resonance energy $\omega_l$ in Eq. (7) has also been varied according to the prediction of the hydrodynamic model, or assumed to be at $\omega_l = 20$ MeV for all $3 \leq l \leq 6$. The shaded area in Fig. 1 indicates the range investigated in the analysis. As is apparent, different sets of assumptions have little effect on the extracted dipole and quadrupole form factors at low momentum transfer $(q \leq 1.2$ fm$^{-1})$, and the uncertainties in the

dipole and quadrupole strength introduced by the different assumptions are $\pm 7\%$ and $\pm 15\%$, respectively.

After subtracting the transverse contributions, the energy dependence of electric dipole $g_1(\omega)$, electric quadrupole $g_2(\omega)$, and the sum of higher multipole excitation functions $g_\Sigma(\omega)$ have been obtained by the method described earlier and the results are shown in Figs. 2 and 3. The smooth curves are obtained by overlapping with another expansion shifted by 175 keV energy bins. The reduced $\chi^2$ for the curves is of the order of unity. The errors indicated occasionally are the errors associated with the least square method. The absence of the excitation curves for $^{44}$Ca above 27 MeV results from the fact that the spectra above this energy were not measured in some cases. The integrated form factors for each multipole excitation are shown in Fig. 4.

## IV. DISCUSSION

### A. Giant dipole resonance (GDR)

The present results have revealed considerable structure in the GDR over a wide range of excitation energy in $^{42}$Ca and $^{44}$Ca, in contrast to a single-peaked GDR in $^{40}$Ca.[1] The dipole peaks have been observed at various energies between 9 and 28 MeV in both nuclei, with at least two regions of gross structure. As is seen in Figs. 2, 3, and 5, these bumps are relatively broad and the centroid energies obtained by fitting to two Breit-Wigner shapes are 17.8 and 23.0 MeV in $^{42}$Ca, 16.2 and 21.3 MeV in $^{44}$Ca. The observed positions of the dipole resonances, the reduced transition probabilities $B(C1)$, and the percentage depletion of the isovector EWSR are shown in Table II. The dipole strengths integrated up to 22 MeV in both $^{42}$Ca and $^{44}$Ca exhaust the isovector dipole ESWR (classical dipole sum rule) and exceeds by 70% when integrated up to 35 MeV excitation energy. The obtained strength of the GDR's is comparable to the measured total photoabsorption cross section for $^{40}$Ca,[1] where the classical dipole sum is exhausted approximately at 26 MeV and exceeds by 50% at 47 MeV in excitation energy.

### 1. Effects of isospin splitting

The splitting of the GDR in medium-weight nuclei with the ground state isospin $T_0 > 0$ has largely been explained by the isospin effect.[33] The

TABLE I. The total form factors integrated from 10 to 25 MeV and the transverse excitation contributions. $a$ and $b$ are parameters of spectral shape of the transverse excitation $|W_T|^2 = a\omega + b$. Also shown is the ratio of the transverse components to the total strength. Errors in the total form factors are $\pm 4\%$.

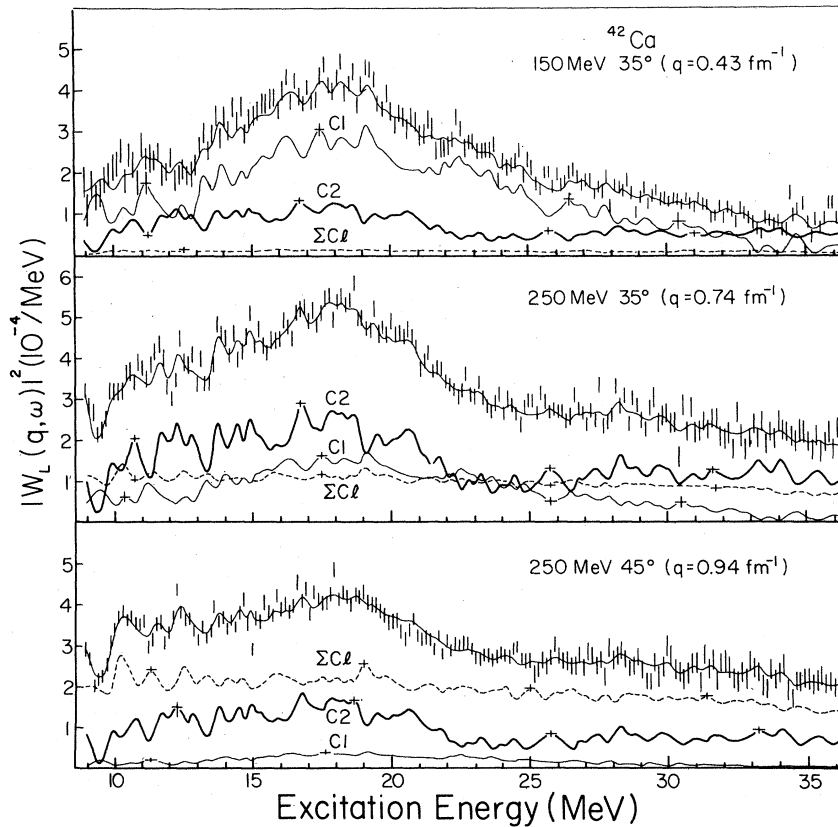| E (MeV) | $\theta$ (deg) | $\|F\|^2$ ($10^{-3}$) | $\|F_{tr}\|^2$ ($10^{-3}$) | $a$ ($10^{-6}$/MeV) | $b$ ($10^{-5}$/MeV) | $\left[1/2 + \tan^2\dfrac{\theta}{2}\right]\|F_{tr}\|^2/\|F\|^2$ (%) |
|---|---|---|---|---|---|---|
| | | | $^{42}$Ca | | | |
| 150 | 35 | 5.02 | 0.47 | 2.2 | -1.97 | 5.8 |
| 183 | 35 | 6.37 | 0.74 | 2.2 | -0.89 | 7.2 |
| 250 | 35 | 7.56 | 1.30 | 2.2 | 1.30 | 11.1 |
| 250 | 45 | 6.49 | 1.10 | 2.5 | 0.60 | 11.9 |
| 250 | 55 | 5.30 | 0.62 | 2.8 | -1.78 | 9.3 |
| | | | $^{44}$Ca | | | |
| 124 | 35 | 4.70 | 0.37 | 0.84 | 0.0 | 4.8 |
| 150 | 35 | 5.31 | 0.47 | 2.2 | -2.00 | 5.2 |
| 183 | 35 | 5.91 | 0.74 | 2.2 | -0.89 | 7.8 |
| 250 | 35 | 7.33 | 1.30 | 2.2 | 1.30 | 11.4 |
| 250 | 42 | 7.39 | 1.20 | 2.4 | 0.97 | 11.2 |
| 250 | 50 | 5.28 | 0.80 | 2.6 | -0.78 | 11.3 |



FIG. 2. The longitudinal differential form factor of $^{42}$Ca at various momentum transfers. The error bars show the experimental results sorted by 150 keV. The thin curve, thick curve, and dashed curve show the dipole, quadrupole, and higher multipole ($3 \le Cl \le 6$) excitations, respectively. Also shown is the sum of the all multipole excitations by thin curve. The occasional error bars on the curves indicate errors associated with the least square method.
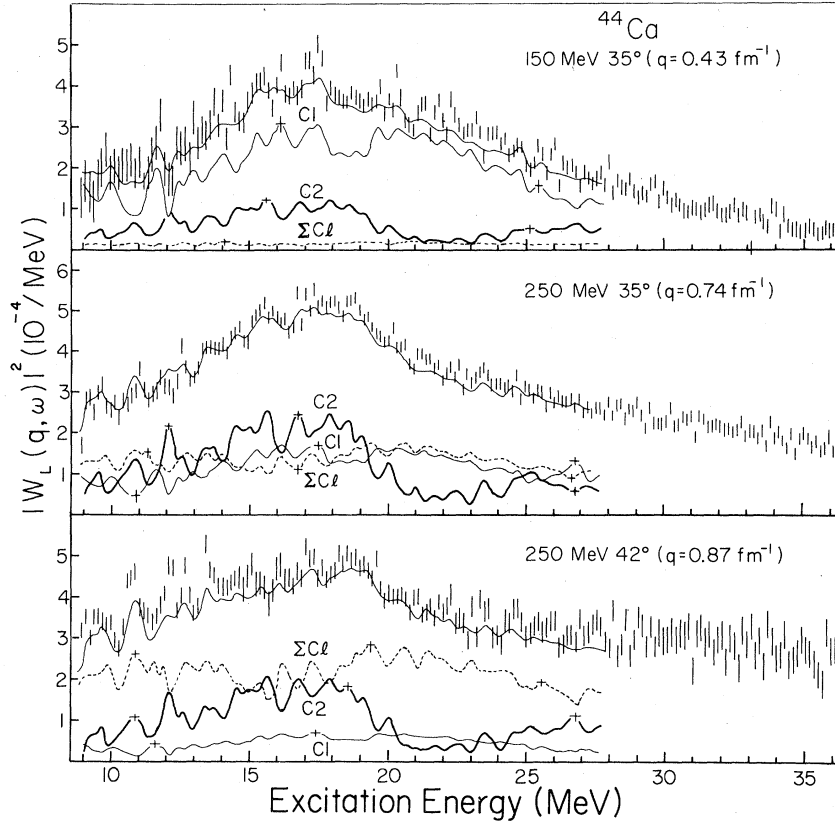
FIG. 3. The longitudinal differential form factor of $^{44}$Ca at various momentum transfers. See caption of Fig. 2.

theory predicts[10] that the GDR may split into two peaks corresponding to the isospin $T_< = T_0$ and $T_> = T_0 + 1$, with the separation energy of

$$\Delta\omega = \omega(T_>) - \omega(T_<) = U_D \left[ 1 + \frac{1}{T_0} \right], \qquad (9)$$

where $U_D = 60 T_0 / A$ (MeV) is the effective symmetry energy for the dipole state. The relative strength of the two states is given by

$$\frac{|C_>|^2}{|C_<|^2} = \frac{\int |W_L^>(q,\omega)|^2 d\omega}{\int |W_L^<(q,\omega)|^2 d\omega}$$

$$\approx \frac{1}{T_0} \frac{1 - 1.5 T_0 / A^{2/3}}{1 + 1.5 / A^{2/3}}. \qquad (10)$$

For the calcium isotopes, the ratios of the strength of the $T_>$ resonance to that of the $T_<$ resonance are 0.76 for $^{42}$Ca ($T_0 = 1$) and 0.34 for $^{44}$Ca ($T_0 = 2$). Equation (9) leads to the energy splittings of 2.9 MeV for $^{42}$Ca and 4.1 MeV for $^{44}$Ca.

As is seen in Fig. 5, the comparable strengths of the two peaks in $^{44}$Ca is not explainable by the prediction, and the obtained splitting energies of 5.2 MeV in $^{42}$Ca and 5.1 MeV in $^{44}$Ca by fitting to two Breit-Wigner shapes are also not in agreement with the theory.

Similar features of the splitting into the isospin states in $^{42}$Ca were also obtained by Diener et al.[9] in a particle-hole model calculation using Kuo-Brown $G$ matrix, although both components are fragmented into a number of states. As shown in Fig. 5, their calculation indicates that the $T_< = 1$ state is concentrated around 17 MeV with smaller peaks at 20 and 23 MeV, while $T_> = 2$ strength is shared by two states at 19.3 and 19.9 MeV. The dipole strength ratio of the sum of $T_<$ and $T_>$ states and the splitting energy are in close agreement with the phenomenological prediction of Eqs. (9) and (10).

In Fig. 6, the present results on the dipole resonances are compared with the $^{42}$Ca $(\gamma,p)$,[5,6] $^{42}$Ca$(\gamma,n)$,[7] and $^{44}$Ca$(\gamma,p)$,[8] as well as with the
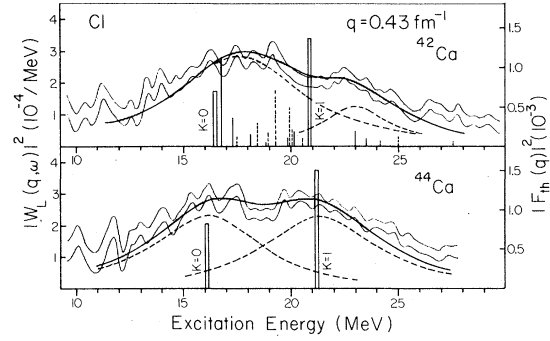
FIG. 5. The longitudinal dipole differential form factors of $^{42}$Ca and $^{44}$Ca at $q = 0.43$ fm$^{-1}$. The shaded area shows the errors arising from the least square method. The two gross resonances in both isotopes are fitted by two Breit-Wigner shape cross sections. The $K$ splitting of the Suzuki-Rowe model (Refs. 40 and 42) is compared with the spectra. Shell model calculation (Ref. 9) is also shown by solid lines for the $T_<$ state and dashed lines for the $T_>$ state. Both $T_<$ and $T_>$ strengths are multiplied by a factor of 2.

FIG. 4. The longitudinal form factors integrated from 10 to 25 MeV for $^{42}$Ca and $^{44}$Ca, together with the result of the multipole expansion. The dashed, dash-dotted, and long dashed curves are the $C1$, $C2$, and $\Sigma Cl$ ($l \geq 3$) components, respectively. The solid curve is the sum of the all multipole excitation. The occasional error bars on the $C1$, $C2$, and $\Sigma Cl$ ($l \geq 3$) curves include statistical error and model dependence of the higher multipole excitations.

$^{44}$Ca$(\gamma, n)$ cross section derived from the measurement for the natural calcium.[34] The Goldhaber-Teller model was used to convert these photoreaction cross sections to the point $q = 0.43$ fm$^{-1}$. Since proton or neutron emission is the major decay mode of the GDR, the sum of these cross sections should be close to the dipole spectra obtained by the electron scattering experiment. As is seen in Fig. 6, the magnitudes of the photonuclear cross sections in $^{42}$Ca are considerably smaller than the result obtained in the present work. Our result for

TABLE II. Reduced transition probabilities $B(C1, \uparrow)$ obtained by the multipole expansion and the depletion of the isovector electric dipole EWSR $(S_1)$. The positions of dipole peaks are indicated in square brackets. Errors in $B(C1)$ and $S_1$ are $\pm 10\%$, which include errors arising from the model dependence on the higher multipole transitions.

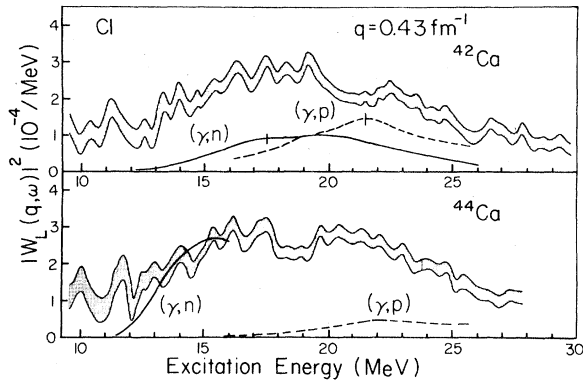| $^{42}$Ca | | | $^{44}$Ca | | |
|---|---|---|---|---|---|
| $\omega$ (MeV) | $B(C1)$ $(e^2 \text{fm}^2)$ | $S_1$ (%) | $\omega$ (MeV) | $B(C1)$ $(e^2\text{fm}^2)$ | $S_1$ (%) |
| 9.0~12.5 [9.4, 11.2] | 1.49 | 10.2 | 9.0~12.1 [10.0, 11.7] | 1.46 | 9.4 |
| 12.5~14.5 [13.3, 13.9] | 1.34 | 11.5 | 12.1~14.5 [13.0, 14.1] | 1.60 | 13.3 |
| 14.5~18.0 [16.2, 17.5] | 3.06 | 31.9 | 14.5~18.5 [15.3. 16.2, 17.3] | 3.78 | 38.4 |
| 18.0~21.0 [18.3, 19.2] | 2.81 | 35.1 | 18.5~23.0 [19.6, 20.3, 21.4, 22.0] | 4.33 | 55.3 |
| 21.0~26.0 [22.5] | 3.19 | 48.1 | 23.0~25.0 [22.9] | 1.52 | 22.4 |
| 26.0~30.0 [26.7] | 1.39 | 25.0 | 25.0~27.0 | 0.96 | 15.3 |
| 30.0~35.0 | 0.64 | 13.3 | | | |
| 10.0~25.0 | 11.0 | 129 | 10.0~25.0 | 12.2 | 138 |
| 9.0~35.0 | 13.9 | 173 | | | |

FIG. 6. The longitudinal dipole differential form factors of $^{42}$Ca and $^{44}$Ca at $q =0.43$ fm$^{-1}$ are compared with photoreaction cross sections. See caption of Fig. 5. The $^{42}$Ca $(\gamma,p)$ (Ref. 6), $^{42}$Ca $(\gamma,n)$ (Ref. 7), $^{44}$Ca $(\gamma,p)$ (Ref. 8), and $^{44}$Ca $(\gamma,n)$ (Ref. 34) cross sections were converted to the point $q =0.43$ fm$^{-1}$.

$^{42}$Ca indicates that there should be more dipole strength at the excitation energy less than 20 MeV, which probably decay by emitting neutrons. In $^{44}$Ca the result shows that a considerable dipole strength is missing at the higher excitation energy above 16 MeV, which suggests that the major part of the GDR in $^{44}$Ca would decay through the neutron channel. It is noted that some dipole strength observed below $(\gamma,n)$ threshold may relate to $\gamma$ and $\alpha$ decay cross sections.

In the medium-weight nuclei, the major part of the $(\gamma,n)$ and $(\gamma,p)$ cross sections are known to represent $T_<$ and $T_>$ states, respectively.[8,35] The ratio of the bremsstrahlung-weighted cross section

$\sigma_{-1}$ of the $(\gamma,p)$ and the $(\gamma,n)$ cross sections in 1.23 for $^{42}$Ca. However, if we assume that the observed strength centered at approximately 18 MeV is due to neutron decay in $^{42}$Ca, the ratio becomes 0.52, which is in closer agreement with the value of 0.76 predicted by Eq. (10). For $^{44}$Ca, if we assume that the result of subtracting the proton decay cross section from the total dipole spectrum is all neutron decay cross section, the ratio would be 0.09. These numbers correctly reflect the trend of the prediction that the ratio of the $T_>$ over $T_<$ decreases with increasing neutron numbers.

The centroid energies of the proton and the neutron decay cross sections were obtained at $q =0.43$ fm$^{-1}$ by

$$\bar{\omega} = \frac{\int \omega \mid W_L(q,\omega) \mid^2 d\omega}{\int \mid W_L(q,\omega) \mid^2 d\omega}. \tag{11}$$

The splitting energies and the ratio of the strength of the $T_>$ and $T_<$ states, as well as the predictions of the isospin splitting theory, are given in Table III. The obtained splitting energies are in fair agreement with the predictions. The results of the present discussion may be changed to some extent by the fact that some part of the proton decay cross section may be $T_<$ state, while a small amount of the neutron decay cross section may be $T_>$ state.[8,35] In addition, the cross sections of the other decay channels such as $(\gamma,2n),(\gamma,pn)$ were ignored in the present discussion. However, from the above discussion the gross resonance structures around 21 MeV in $^{44}$Ca appear to be made up from an appreciable amount of the $T_<$ component.

TABLE III. Comparison of the gross structures of the giant resonance with isospin splitting theory. The predictions of the theory are shown in square brackets.

|        | $\omega(T_<)$ (MeV) | $\omega(T_>)$ (MeV) | $\Delta\omega$ (MeV) | $\dfrac{C\mid_>\mid^2}{\mid C_<\mid^2)}$ |
|--------|---------------------|---------------------|----------------------|------------------------------------------|
| $^{42}$Ca | 19.6 $(\gamma,n)$[a] | 21.6 $(\gamma,p)$[b] | 2.0 | 1.23 |
|        | 17.3 (present) |  | 4.3 | 0.52 |
|        |  |  | [2.9] | [0.76] |
| $^{42}$Ca | 18.3 (present) | 22.0 $(\gamma,p)$[c] | 3.7 | 0.09 |
|        |  |  | [4.1] | [0.34] |

[a]Evaluated from the data of Ref. 7.
[b]Evaluated from the data of Refs. 5 and 6.
[c]Evaluated from the data of Ref. 8.

The study of the $^{41}$K$(p,\gamma_0)^{42}$Ca reaction also revealed[9] two peaks at 17.4 and 20.4 MeV in the gross GDR structure, and each peak was assigned as $T_<$ and $T_>$ states, respectively. The energy difference of these two peaks is in good agreement with the isospin splitting theory, but the observed strength ratio of 6.6 in favor of the upper peak is not. The lower peak observed in the $^{41}$K$(p,\gamma_0)^{42}$Ca reaction may correspond to the peak cross section around 18 MeV in the present spectra, where the presence of the large neutron decay channel is inferred. The existence of the 20.4 MeV peak is not evident in the present result. This could arise from the fact that the ground state $\gamma$ transition amounts to only 8% of the classical dipole sum rule, while the currently obtained spectra essentially correspond to the total photoabsorption cross section scaled by the $C1$ form factor. In the $^{44}$Ca$(\gamma,p_0)$ reaction, two peaks were also observed at 17.5 and 21.3 MeV.[8] The separation energy of these peaks roughly agrees with the isospin splitting theory, but the intensity ratio is again 1.3 in favor of the upper peak. It is noted that both the $^{42}$Ca$(\gamma,p_{\rm total})$ (Refs. 5,6) and the $^{44}$Ca$(\gamma,p_{\rm total})$ (Ref. 8) cross sections exhibit totally different shapes from the $(\gamma,p_0)$ reactions.

### 2. Effects of nuclear deformation

The low-lying structure in the calcium isotopes has been successfully explained by the mixtures of a prolately deformed core-excited rotational band and $(fp)^n$ configurations.[36,37] Inelastic $\alpha$-scattering data showed[38] that the admixtures of the deformed components in the ground states of $^{42}$Ca and $^{44}$Ca are 30%, in contrast to those of 10% and 4% in $^{40}$Ca and $^{48}$Ca, respectively. These studies may suggest that the nuclear deformation plays an important role even in the high-lying giant resonance regions in $^{42}$Ca and $^{44}$Ca.

The form factors for the first $2^+$ states were also measured in the present experiment, and $B(E2,\uparrow)=(470\pm23)$ $e^2$ fm$^4$ for $^{42}$Ca (Ref. 26) and $(658\pm60)$ $e^2$ fm$^4$ for $^{44}$Ca were obtained by DWBA analysis. In the rotational picture the deformation parameter $\beta_2$ is related to the reduced transition probability $B(E2)$ by

$$\beta_2=\frac{4\pi}{3}\,\frac{1}{ZR_0^2}[B(E2,\uparrow)]^{1/2}. \tag{12}$$

Using the currently obtained $B(E2)$ values, the $\beta_2$'s were found to be 0.241 for $^{42}$Ca and 0.276 for

$^{44}$Ca, respectively. These $\beta_2$ values are comparable to those of 0.234 for $^{42}$Ca and 0.258 for $^{44}$Ca, which Träger obtained[39] recently from the charge distributions of the calcium isotopes measured by laser spectroscopy. The intrinsic quadrupole moment is also related to the deformation parameter by

$$Q_0=\frac{3}{\sqrt{5\pi}}\,Z\,R_0^2\,\beta_2, \tag{13}$$

which leads to $(0.69\pm0.04)$ b and $(0.81\pm0.08)$ b for $^{42}$Ca and $^{44}$Ca, respectively. These quadrupole moments can be considered to arise from the core-excited deformed state and $(fp)^n$ configurations. It is noted that Towsley et al. deduced[37] the intrinsic quadrupole moment of $\sim1.25$ b for the complex states in $^{42}$Ca ( the lowest $K=0^+$ band, starting from the 1.84 MeV, $0^+$ state) from the known $B(E2)$ values for the inband and the interband transitions between the $(fp)^n$ dominant and the deformed complex states in the framework of the coexistence model.

Based on the vibrating potential model (VPM), Suzuki and Rowe predict[40] a splitting of the GDR into $K=0$ and $K=1$ resonances for deformed nuclei. The resonance energy $\omega_K$ in the VPM is given by

$$\omega_{K=0}\approx 80/A^{1/3}(1-\tfrac{2}{3}\delta)$$

and    (14)

$$\omega_{K=0}\approx 80/A^{1/3}(1-\tfrac{2}{3}\delta),$$

where $\delta=0.95\beta_2$. We find the $K$-splitting energies to be 5.2 MeV in $^{42}$Ca and 5.9 MeV in $^{44}$Ca. The classical hydrodynamic model gives[41] a similar splitting energy by the relation of $0.861\beta_2\omega_{(K=0)}$, based on the static deformation of the ground state.

By applying a model independent sum rule, Suzuki and Rowe have also shown[42] that the dipole transition charge density is expressed in terms of $\beta_2$ via the relation

$$\rho_{\rm tr}(r)\propto\frac{d\rho_0}{dr}+\frac{\kappa}{\sqrt{5}}\left[\frac{d}{dr}+\frac{3}{r}\right]\rho_2(r), \tag{15}$$

where

$$\rho_0(r)=\sqrt{4\pi}\left[1+\frac{1}{8\pi}\frac{\langle r^{-2}\rangle}{\langle r^{-1}\rangle}\,|\beta_2|^2c_0^2\frac{\partial}{\partial r}\right.$$

$$\left.+\frac{1}{4\pi}\,|\beta_2|^2c_0^2\frac{\partial^2}{\partial r^2}+\cdots\right]\rho_{\rm gr}(r)$$

$$\rho_2(r) = \left[ -\beta_2 c_0 \frac{\partial}{\partial r} \right.$$

$$\left. + \frac{1}{7} \left[ \frac{5}{4\pi} \right]^{1/2} \beta_2^2 c_0^2 \frac{\partial^2}{\partial r^2} + \cdots \right] \rho_{gr}(r),$$

and $\kappa = 2$ for $K = 0$, $-1$ for $K = 1$ mode. The strengths of the $K = 0$ and $K = 1$ resonances is given in the Born approximation by

$$F_L(q) = \frac{\sqrt{4\pi}}{Z} \left[ \frac{2}{1+\delta_{K0}} \right]^{1/2} \frac{1}{[24mA\omega_K]^{1/2}}$$

$$\times q \left[ \int \rho_0(r) j_0(qr) r^2 dr \right.$$

$$\left. - \frac{\kappa}{\sqrt{5}} \rho_2(r) j_2(qr) r^2 dr \right]. \qquad (16)$$

The positions and the strengths of the $K = 0$ and $K = 1$ states at $q = 0.43$ fm$^{-1}$ are compared with the dipole spectra in Fig. 5. Since the factor $80/A^{1/3}$ in Eq. (14) may be larger in the region of $A \sim 40$ (Ref. 43), we used 19.5 MeV for this factor which is the peak position of the GDR in $^{40}$Ca. The predicted splitting energies are large enough to explain the observed broadening; however, the strength for the $K = 1$ mode is predicted to be larger than that of the $K = 0$ mode. This situation is also encountered in the classical hydrodynamic model.[41]

The splitting of the GDR in heavy deformed nuclei has been explained by the dynamic colective model (DCM),[44] where the surface vibrations and rotations are coupled to the dipole oscillation. The existence of the rotational structures, and the relatively large strength of the transition probabilities of the first $2^+$ states in the calcium isotopes may suggest the presence of coupling effects to the GDR. In the DCM an approximate splitting energy $\Delta\omega_K$ between the $K = 0$ and $K = 1$ modes for the calcium isotopes is given by[45]

$$\Delta\omega_K \sim (\hbar\omega_1 - \hbar\omega_0) + \frac{\sqrt{2}}{2} E_\gamma, \qquad (17)$$

where

$$\hbar\omega_1 = 70/A^{1/3}(1 + 0.290\beta_2 + 0.092\beta_2^2 + \cdots),$$

$$\hbar\omega_0 = 70/A^{1/3}(1 - 0.580\beta_2 + 0.366\beta_2^2 + \cdots).$$

The $\gamma$-vibrational energy $E_\gamma$ is taken to be the energy of the first $2^+$ state in the $K = 2^+$ band. Comparison of the low-lying structure in $^{42}$Ca with

$^{40}$Ca has shown [37] that the $2^+$, $K = 2^+$ state is most likely at 3.39 MeV in $^{42}$Ca, and the similar structure of the low-lying states in $^{42}$Ca and $^{44}$Ca suggests that nearly the same energy could be used for $^{44}$Ca. We find the $K$-splitting energies to be 5.6 MeV for $^{42}$Ca and 6.0 MeV for $^{44}$Ca, which are about the same magnitude as the predictions of the VPM.

One of the most prominent features of the DCM is the splitting of the $K = 1$ state into $S = 1$ and $S = -1$ states, reflecting the occurrence of a dynamic triaxiality in the GDR. The splitting energy $\Delta\omega_s$ between $S = 1$ and $S = -1$ states is given by[45]

$$\Delta\omega_s(K = 1) \approx \hbar\omega_1 G_2(3K)^{1/2} \left[ \frac{2\epsilon}{E_\gamma} \right]^{1/2} \beta_2, \qquad (18)$$

where $\epsilon = \hbar^2/2\mathcal{J}_0$ and $G_2$ is a function of $\beta_2$. Using 0.095 MeV for $\epsilon$,[36,37] we find the splitting energies of the $K = 1$ state to be 1.7 MeV in $^{42}$Ca and 2.0 MeV for $^{44}$Ca. The relative dipole strength of the $K = 1$ to the $K = 0$ state in the DCM is reduced to[46]

$$\frac{B(K = 0 \to 1, S = 0 \to \pm 1)}{B(K = 0 \to 0, S = 0 \to 0)}$$

$$\approx \frac{2(-0.654 + 0.114\beta_2 - 0.14\beta_2^2)^2}{(0.925 + 0.33\beta_2 + 0.323\beta_2^2)^2}$$

$$\times \frac{[\sqrt{2}/4\Gamma(\sqrt{2}/4)]^2}{\Gamma[(\sqrt{2}+2)/2]}, \qquad (19)$$

which gives the ratio of 0.67 for $^{42}$Ca and 0.65 for $^{44}$Ca. These features obtained in the DCM are about the same as those found in the calculations for heavy deformed nuclei.[44]

In summary, the current available theories such as the VPM and the DCM predict the $K = 0$ and $K = 1$ resonances in the GDR to split by approximately 6 MeV, if they are applied to the calcium isotopes. The strength of the $K = 1$ state is generally predicted to be larger than that of the $K = 0$ state. The comparison of the theory with the observed dipole spectra, therefore, suggests that the gross resonance structure in $^{44}$Ca may reflect the effect of nuclear deformation; however, the origin of the broadening observed in $^{42}$Ca is not apparent. It is also worth mentioning that two resonance structures of the GDR were also observed in some of the titanium isotopes.[5]

## B. Giant quadrupole resonance (GQR)

The GQR's are well separated in the present analysis over the whole excitation energy region

currently investigated. The collective part of the quadrupole resonance located between 10 and 22 MeV is regarded as isoscalar type. The strength in this energy region exhausts the isoscalar EWSR by $(61\pm9)\%$ in $^{42}$Ca and $(46\pm7)\%$ in $^{44}$Ca. As is seen in Figs. 2 and 3, the GQR in these nuclei consists of several clusters of quadrupole states. The observed positions and the strengths of these clusters are summarized in Table IV. In contrast to the GQR's in heavy nuclei, which are generally concentrated in a narrow energy range of a few MeV,[4] the GQR's in the calcium isotopes are broad and split into several clusters. Similar broadening and clustering of the GQR has been observed in the sd-shell nuclei.[14,47] However, the GQR's in the calcium isotopes appear to have a narrower width than those in sd-shell nuclei and retain some characteristics of those in the heavier nuclei. The centroid energies of the GQR calculated by Eq. (11) are 16.0 MeV in $^{40}$Ca, 16.3 MeV in $^{42}$Ca, and 15.4 MeV in $^{44}$Ca, and their total widths (FWHM) span approximately 7.0 MeV in $^{40}$Ca, 11 MeV in $^{42}$Ca, and 7.5 MeV in $^{44}$Ca.

The obtained quadrupole cross sections are compared with the result for $^{40}$Ca in Fig. 7. It is noted that the result of the electron scattering experiment on $^{40}$Ca shows a broader quadrupole resonance than the result of the inelastic hadron scattering where the GQR was reported to be concentrated at $(18\pm0.3)$ MeV with a width of $(3.5\pm0.3)$ MeV.[4,11]

The splitting of the isoscalar GQR has been observed in heavy deformed nuclei,[48] and the VPM also predicts[40] that the isoscalar GQR be split into
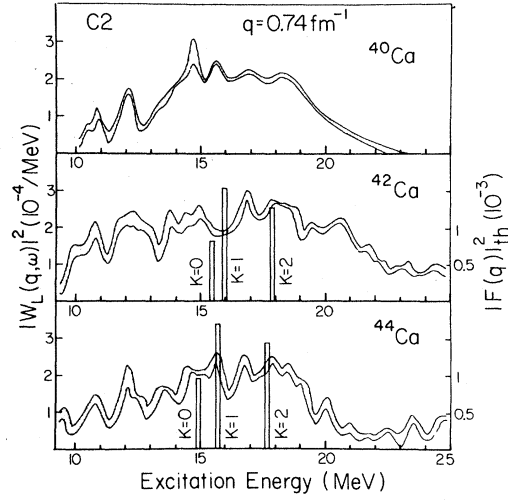


FIG. 7. The longitudinal quadrupole differential form factors of $^{42}$Ca and $^{44}$Ca at $q=0.74$ fm$^{-1}$ are compared with the result of $^{40}$Ca (Ref. 3). The shaded area for $^{40}$Ca was obtained by combining the result of $^{40}$Ca at $q=0.67$ fm$^{-1}$ and $q=0.81$ fm$^{-1}$, while those of $^{42}$Ca and $^{44}$Ca show the errors arising from the least square method. The $K$ splitting of the Suzuki-Rowe model is also shown.

$K=0$, 1, and 2 modes. The eigenfrequencies of each state are given by

$$\omega_{K=0}=\sqrt{2}\hbar\omega(1-\tfrac{1}{3}\delta),$$

$$\omega_{K=1}=\sqrt{2}\hbar\omega(1-\tfrac{1}{6}\delta), \tag{20}$$

$$\omega_{K=2}=\sqrt{2}\hbar\omega(1+\tfrac{1}{3}\delta),$$

TABLE IV. Reduced transition probabilities $B(C2,\uparrow)$ obtained by the multipole expansion and the depletion of the isoscalar electric quadrupole EWSR ($S_2$), or the isovector quadrupole EWSR ($S_2$, denoted by*). Also shown is the depletion of the isoscalar monopole EWSR ($S_0$). The positions of the quadrupole peaks are given in square brackets. Errors in $B(C2)$ and $S_2$ are $\pm17\%$ which include errors from the model dependence on the higher multipole transitions.

| | $^{42}$Ca | | | | $^{44}$Ca | | |
|---|---|---|---|---|---|---|---|
| $\omega$ (MeV) | $B(C2)$ ($e^2$ fm$^4$) | $S_2$ (%) | $S_0$ (%) | $\omega$ (MeV) | $B(C2)$ ($e^2$ fm$^4$) | $S_2$ (%) | $S_0$ (%) |
| 9.5~11.3 [9.9, 10.8] | 37.5 | 4.0 | (6.1) | 9.5~11.4 [9.6, 10.9] | 31.3 | 3.4 | (5.2) |
| 11.3~13.4 [11.8, 12.2, 12.8] | 62.0 | 7.8 | (11.7) | 11.4~14.1 [12.1, 13.4] | 60.8 | 8.3 | (12.7) |
| 13.4~15.9 [13.7, 14.5, 14.9] | 74.7 | 11.2 | (17.1) | 14.1~16.2 [14.5, 15.7] | 59.7 | 9.7 | (14.8) |
| 15.9~19.2 [16.8, 18.2] | 118 | 21.3 | (32.6) | 16.2~19.6 [16.7, 17.8, 18.6] | 102 | 19.7 | (30.1) |
| 19.2~22.0 [19.5, 20.6] | 81.0 | 17.1 | (26.1) | 19.6~22.0 [20.1] | 23.4 | 5.2 | (8.0) |
| 22.0~25.0 | 41.5 | 9.2* | (14.0) | 22.0~25.0 | 23.6 | 4.9* | (7.5) |
| 25.0~30.0 | 84.4 | 21.8* | (33.3) | 25.0~27.0 | 21.3 | 4.9* | (7.5) |
| 30.0~35.0 | 74.3 | 22.7* | (34.7) | | | | |
| 10.0~22.0 | 373 | 61.4 | | 10.0~22.0 | 277 | 46.3 | |
| 22.0~35.0 | 200 | 53.7* | | | | | |

where $\sqrt{2}\hbar\omega \approx 58/A^{1/3}$ MeV. The strengths for each state were also obtained in a similar way to

$$F_L(q) = \frac{1}{2Zm\,[S(2,0)\omega_{K=0}]^{1/2}}\,q\left\{\int\rho_0(r)j_1(qr)r^3dr + \frac{1}{7\sqrt{5}}\int\rho_2(r)[7j_1(qr)-3j_3(qr)]r^3dr\right\}, \tag{21}$$

where

$$S(2,0) = \frac{5A\langle r^2\rangle}{4\pi m}\left[1 + \frac{Q_0}{2A\langle r^2\rangle}\right].$$

The measured mean square radii are 3.51 fm for both isotopes.[19] The calculated positions and the strengths at $q=0.74$ fm$^{-1}$ are compared with the observed quadrupole spectra in Fig. 7.

The predicted splitting energies betwen $K=0$ and $K=2$ states are 2.5 MeV for $^{42}$Ca and 2.8 MeV for $^{44}$Ca. As is seen in Fig. 7, the predicted positions are confined to a rather narrow region, contrary to the broad quadrupole spectra.

Very recently the study of the inelastic scattering of $^6$Li particles has also revealed[12] the broadening of the GQR in $^{42}$Ca and $^{44}$Ca as compared with those in $^{40}$Ca and $^{48}$Ca. The observed broadening was analyzed in terms of the overlapping resonances of each $K$ state. The currently obtained quadrupole spectra, however, indicate the presence of more structure due to clustering of GQR states in the calcium isotopes.

Some possibilities also exist for the excitation of the monopole resonance among the currently assigned quadrupole resonances at the low-energy side of the GQR, since various microscopic calculations predict the presence of the monopole resonance in $^{40}$Ca at 13.7 (Skyrme II) or 16.5 MeV (Skyrme I),[49] at 14 MeV,[50] and around 16 MeV as well as at higher excitation energies.[51] No definite evidence of the monopole state was seen in a recent forward-angle measurement of $\alpha$-particle scattering in $^{40}$Ca,[52] although some evidence for the weak monopole resonance (8% of EWSR) was reported at the same excitation energies of the GQR in a $^3$He-scattering experiment.[53] In Table IV the monopole strengths are also given for each cluster.

In addition to the isoscalar GQR, the monotonic quadrupole excitations were separated above 22 MeV, as is seen in Figs. 2 and 3. These quadrupole resonances are considered a part of the isovector quadrupole resonance, which is known to lie at $120-130/A^{1/3}$ MeV in medium and heavy nuclei.[4,54] It seems that the isovector quadrupole resonances in the calcium isotopes are too broad to be observed as a single resonance.

the GDR.[42] The form factor for the $K=0$ mode, for example, is given here:

## C. Higher multipole excitations and nuclear continuum

As is seen in Figs. 2, 3, and 8, the higher multipole excitations are a major part of the whole spectra at higher momentum transfer. They consist of several resonances between 9 and 25 MeV and a continuum spectra over the entire excitation energy range presently studied. In order to extract the resonant part in the spectra, the following phenomenological shape has often been used[3] for the shape of continuum

$$|W(q,\omega)|^2 = \alpha(\omega-\omega_0)^{1/n}, \tag{22}$$

where $\omega_0$ is the threshold energy of particle emission, $\alpha$ and $n$ are fitting parameters to be adjusted to the continuum spectra above the resonance region. In our earlier paper[3] the validity of the phenomenological shape of Eq. (22) was investigated in a framework of a shell model including isovector quadrupole, octupole, and all other higher multipole transitions. It was shown that Eq. (22) is a quite reasonable approximation. It should be also noted that such phenomenology is used in the work of hadron scattering.[4]

An attempt was made here to obtain the strength of the higher multipole transition assuming the shape of Eq. (22) for the continuum, as is shown in Fig. 8. The strengths of the resonant part of the higher multipole transitions deplete $30-45\%$ of the isoscalar octupole EWSR, although some parts of these resonances may be $C4$ and $C5$ transitions. The obtained strength and the distribution of the higher multipole resonance in $^{42}$Ca and $^{44}$Ca appear to be very similar to those[3] in $^{40}$Ca, and it is concluded that the octupole resonances in the calcium isotopes are spread over a broader energy region than for medium and heavy nuclei.[55]

Highly excited octupole states in $^{40}$Ca have been calculated using microscopic models.[49-51,56] These calculations also predict fragmentation of the octupole states between 8 and 45 MeV. For instance, Hammerstein et al.[50] predicted a strength of $2.1\times10^3$ $e^2$ fm$^6$ for the isoscalar octupole, and $6.4\times10^3$ $e^2$ fm$^6$ for the isovector octupole resonance. Krewald and Speth[51] calculated $5.1\times10^3$
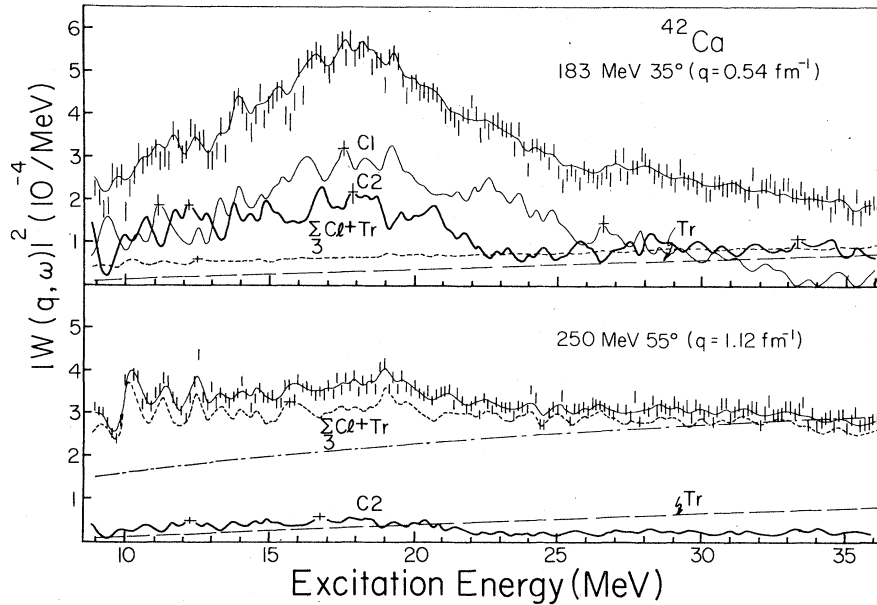
FIG. 8. The total differential form factor of $^{42}$Ca at 183 MeV 35° and 250 MeV 55°. The short-dashed curve is the sum of the transverse excitations (labeled $T_r$) and the higher multipole ($l \geq 3$) excitations. The dot-dashed curve in the lower figure indicates the phenomenological shape for the continuum, which was used to deduce the resonant part of the octupole strength. The contribution of the dipole strength to the spectra at 250 MeV 55° is negligibly small.

$e^2$ fm$^6$ for the octupole transition. These values are consistent with the present result of $\approx 1.0 \times 10^4$ $e^2$ fm$^6$ for the octupole strength derived using Eq. (22). However, the underlying continuum, which may contain octupole transitions, should be taken into account for complete comparison.

## V. SUMMARY

The spectra of inelastic electron scattering at the momentum transfers between 0.43 and 1.13 fm$^{-1}$ were decomposed into dipole, quadrupole, and other higher multipole transitions using the least square method. The giant dipole resonances in both nuclei have widths of approximately 12 MeV, considerably broader than those of $^{40}$Ca. The dipole strength exceeds the EWSR when integrated up to 22 MeV. In addition, at least two gross resonance structures were observed in both $^{42}$Ca and $^{44}$Ca. These gross structures can be consistently explained by the isospin splitting theory when the present data is combined with the photoreaction results, suggesting that the $T$-lower excitations dominate even in the upper resonance region in $^{44}$Ca. From the comparison with the Suzuki-Rowe model and the dynamic collective model, it is suggested that the splitting of the GDR observed in

$^{44}$Ca is most likely due to the nuclear deformation. However, the origin of the broadening of the GDR observed in $^{42}$Ca is not clear.

The GQR is distributed over a broad excitation region in both $^{42}$Ca and $^{44}$Ca, with the centroid energies at 16.3 MeV in $^{42}$Ca and 15.4 MeV in $^{44}$Ca. The quadrupole resonance spans approximtely 11 MeV in $^{42}$Ca and 7.5 MeV in $^{44}$Ca, with splitting into several clusters. The strengths of the GQR deplete the isoscalar EWSR by $(61 \pm 9)\%$ in $^{42}$Ca and $(46 \pm 7)\%$ in $^{44}$Ca. The clustering of the GQR suggests the possible effects of nuclear deformation on the quadrupole resonance; however, the observed quadrupole resonances are distributed over broader excitation energies than the simple application of the Suzuki-Rowe model, which has been developed primarily for heavy deformed nuclei, suggests. The collective higher multipole resonances $(3 \leq l \leq 6)$ are also found between 10 and 25 MeV excitation energy. If the octupole transitions are assumed for the collective resonant part of the higher multipole resonance, $30-45\%$ of the isoscalar octupole EWSR is exhausted. The major part of the higher multipole resonances, however, forms continuum spectra at and above the giant resonance region.

## ACKNOWLEDGMENTS

[1]J. Ahrens, H. Borchert, K. H. Czock, H. B. Eppler, H. Gimm, H. Gundrum, M. Kröning, P. Riehn, G. Sita Ram, A. Zieger, and B. Ziegler, Nucl. Phys. A251, 479 (1975).

[2]A. Veyssière, H. Beil, R. Bergère, P. Carlos, A. Leprêtre, and A. de Miniac, Nucl. Phys. A227, 513 (1974).

[3]Y. Torizuka, K. Itoh, Y. M. Shin, Y. Kawazoe, H. Matsuzaki, and G. Takeda, Phys. Rev. C 11, 1174 (1975).

[4]F. E. Bertrand, Annu. Rev. Nucl. Sci. 26, 457 (1976).

[5]M. N. Thompson, in Lecture Notes in Physics, edited by B. A. Robson (Springer, New York, 1979), Vol. 92, p. 208; M. N. Thompson et al., in Proceedings of Sendai Conference on Electro- and Photoexcitations, Sendai, Japan, 1977, edited by Y. Kawazoe, Supplement to Research Report of Laboratory of Nuclear Science, Tohoku University, 1977, Vol. 10, p. 241.

[6]R. E. Pywell, M. N. Thompson, K. Shoda, M. Sugawara, T. Saito, H. Tsubota, H. Miyase, J. Uegaki, T. Tamae, H. Ohashi, and T. Urano, Aust. J. Phys. 33, 685 (1980).

[7]Y. I. Assafiri and M. N. Thompson (private communication).

[8]S. Oikawa and K. Shoda, Nucl. Phys. A277, 301 (1977).

[9]E. M. Diener, J. F. Amann, P. Paul, and J. D. Vergados, Phys. Rev. C 7, 705 (1973).

[10]B. Goulard and S. Fallieros, Can. J. Phys. 45, 3221 (1967); R. Ö. Akyüz and S. Fallieros, Phys. Rev. Lett 27, 1016 (1971).

[11]D. H. Youngblood, J. M. Moss, C. M. Rozsa, J. D. Bronson, A. D. Bacher, and D. R. Brown, Phys. Rev. C 13, 994 (1976).

[12]K. T. Knöpfle, A. Sauter, G. J. Wagner, P. Doll, D. L. Hendrie, and H. Wieman, in Proceedings of the International Conference on Nuclear Physics, Berkeley, 1980, Lawrence Berkeley Laboratory Report No. LBL-11118, 1980, p. 262.

[13]M. Sasao and Y. Torizuka, Phys. Rev. C 15, 217 (1977).

[14]Z. M. Szalata, K. Itoh, G. A. Peterson, J. Flanz, S. P. Fivozinsky, F. J. Kline, J. W. Lightbody, Jr., X. K. Maruyama, and S. Penner, Phys. Rev. C 17, 435 (1978).

[15]Y. Torizuka, Y. Kojima, T. Saito, K. Itoh, A. Nakada, S. Mitsunobu, M. Nagao, K. Hosoyama, S. Fukuda, and H. Miura, in Proceedings of the International Conference on Photonuclear Reactions and and Applications, Asilomar, 1973, edited by B. L. Berman (Lawrence Livermore Laboratory, University of California, 1973), Vol. 1, p. 675.

[16]M. Kimura, Y. Torizuka, K. Shoda, M. Sugawara, T. Saito, M. Oyamada, K. Nakahara, K. Itoh, K. Sugiyama, M. Gotoh, K. Miyashita, and K. Kurahashi, Nucl. Instrum. Methods 95, 403 (1971).

[17]J. Friedrich, Nucl. Instrum. Methods 129, 505 (1975). The formula described as set I in this paper was essentially used in the present analysis.

[18]We used computer code TOELS, developed by T. Terasawa and M. Oyamada based on the formula given by D. R. Yennie, D. G. Ravenhall, and R. N. Wilson, Phys. Rev. 95, 500 (1954).

[19]R. F. Frosch, R. Hofstadter, J. S. McCarthy, G. K. Nöldeke, K. J. van Oostrum, M. R. Yearian, B. C. Clark, R. Herman, and D. G. Ravenhall, Phys. Rev. 174, 1380 (1968).

[20]I. Sick and J. S. McCarthy, Nucl. Phys. A150, 631 (1970).

[21]D. Drechsel and H. Überall, Phys. Rev. 181, 1383 (1969).

[22]E. G. Fuller and E. Hayward, in Nuclear Reactions, edited by P. M. Endt and P. B. Smith (North-Holland, Amsterdam, 1962), Vol II, p. 134.

[23]Y. Torizuka, in Proceedings of the International Conference on Nuclear Structure, Tokyo, 1977, edited by T. Marumori (International Academic Printing, Co., Ltd., Tokyo, 1978), p. 397.

[24]K. Itoh, M. Oyamada, and Y. Torizuka, Phys. Rev C 2, 2181 (1970).

[25]M. Croissiaux, R. Hofstadter, A. E. Walker, M. R. Yearian, D. G. Ravenhall, B. C. Clark, and R. Herman, Phys. Rev. 137, B865 (1965).

[26]K. Itoh et al., Research Report of Laboratory of Nuclear Science, Tohoku University, 1974, Vol. 7 (unpublished), p. 15.

[27]P. D. Zimmerman, M. R. Yearian, and T. W. Donnelly, Phys. Rev. Lett. 21, 1392 (1968).

[28]A. Bohr and B. R. Mottelson, Nuclear Structure (Benjamin, New York, 1975), Vol. II, Chap. 6.

[29]J. M. Eisenberg and W. Greiner, Nuclear Models (North-Holland, Amsterdam, 1970), Vol 1, p. 310.

[30]K. Itoh et al., Research Report of Laboratory of Nuclear Science, Tohoku University, Vol. 4, 1971 (unpublished), p. 9.

[31]P. D. Zimmerman, C. F. Williamson, and Y. Kawazoe, Phys. Rev. C 19, 279 (1979).

[32]V. Gillet and E. A. Sanderson, Nucl. Phys. 54, 472 (1964); A91, 292 (1967).

[33]P. Paul, see Ref. 15, Vol. I, p. 407.

[34]J. Goldemberg and L. Katz, Can. J. Phys. 32, 49 (1954).

[35]K. Shoda, H. Miyase, M. Sugawara, T. Saito, S. Oikawa, A. Suzuki, and J. Uegaki, Nucl. Phys. A239, 397 (1975); H. Tsubota, S. Oikawa, J. Uegaki, and T. Tamae, ibid. A303, 333 (1978).

[36]W. J. Gerace and A. M. Green, Nucl. Phys. A93, 110 (1967).

[37]C. W. Towsley, D. Cline, and R. N. Horoshko, Phys. Rev. Lett. 28, 368 (1972); Nucl. Phys. A204, 574 (1973).

[38]M. J. A. de Voigt, D. Cline, and R. N. Horoshko, Phys. Rev. C 10, 1798 (1974).

[39]F. Träger, Z. Phys. 299, 33 (1981); private communication.

[40]T. Suzuki and D. J. Rowe, Nucl. Phys. A289, 461 (1977).

[41]M. Danos, Nucl. Phys. 5, 23 (1958).

[42]T. Suzuki and D. J. Rowe, Nucl. Phys. A292, 93 (1977).

[43]W. D. Myers, W. J. Swiatecki, T. Kodama, L. J. El-Jaick, and E. R. Hilf, Phys. Rev. C 15, 2032 (1977).

[44]J. M. Eisenberg and W. Greiner, see Ref. 29, Vol. 1, p. 331.

[45]M. Danos and W. Greiner, Phys. Rev. 134, B284 (1964).

[46]H. Arenhövel, M. Danos, and W. Greiner, Phys. Rev. 157, 1109 (1967).

[47]K. Itoh, S. Ohsawa, Y. Torizuka, T. Saito, and T. Terasawa, Phys. Rev. C 23, 945 (1981).

[48]H. Miura and Y. Torizuka, Phys. Rev. C 16, 1688 (1977).

[49]G. F. Bertsch and S. F. Tsai, Phys. Rep. 18C, 125 (1975).

[50]G. R. Hammerstein, H. McManus, A. Moalem, and T. T. S. Kuo, Phys. Lett. 49B, 235 (1974).

[51]S. Krewald and J. Speth, Phys. Lett. 52B, 295 (1974).

[52]D. H. Youngblood, in Giant Multipole Resonances, edited by F. E. Bertrand (Harwood Academic, New York, 1980), p. 113; D. H. Youngblood, P. Bogucki, J. D. Bronson, U. Garg, Y.-W. Lui, and C. M. Rozsa, Phys. Rev. C 23, 1997 (1981).

[53]D. Lebrun, M. Buenerd, P. Martin, P. de Saintignon, and G. Perrin, Phys. Lett. 97B, 358 (1980).

[54]R. Pitthan, see Ref. 52, p. 161.

[55]J. M. Moss, D. R. Brown, D. H. Youngblood, C. M. Rozsa, and J. D. Bronson, Phys. Rev. 18, 741 (1978).

[56]S. Shlomo and G. Bertsch, Nucl. Phys. A243, 507 (1975).